

NWP SAF

Satellite Application Facility for Numerical Weather Prediction

Document NWPSAF-EC-VS-011

Version 1.0

20 January 2006

Validation of background error covariances for radiance assimilation

Rheinhold Hess
DWD



Validation of background error covariances for radiance assimilation

Rheinhold Hess
DWD

This documentation was developed within the context of the EUMETSAT Satellite Application Facility on Numerical Weather Prediction (NWP SAF), under the Cooperation Agreement dated 16 December, 2003, between EUMETSAT and the Met Office, UK, by one or more partners within the NWP SAF. The partners in the NWP SAF are the Met Office, ECMWF, KNMI and Météo France.

Copyright 2006, EUMETSAT, All Rights Reserved.

NWP SAF: Visiting Scientist Report

Validation of background error covariances for radiance assimilation

Reinhold Hess (DWD)

Host Institute: ECMWF
Contact Point: Tony McNally
Duration: 9 – 20 January 2006

1 Introduction

It was reported earlier (Hess 2004) that different background error characteristics are detected for different synoptical situations when the NMC–method for background error estimation (Parrish and Derber, 1981) is applied. In brief it has been shown, that generally in case of *bad* weather the forecast errors are much larger with broader correlations than in case of *fair* weather. Useful predictors for *fair* and *bad* weather were vorticity, surface pressure, and windspeed.

In this report the results based on the NMC–method are validated using real observations. For the same periods of *bad* and *fair* weather, that has been used for the previous study, the above results are confirmed using departures (differences between observations and model first guess) of radiosondes and AMSU–A microwave radiances.

Once detected and confirmed, that there are substantial dependencies of background error structure on the actual weather regime, the next step towards an adaptive definition of the errors in a variational context would be to parameterise them depending on suitable predictors. First tests using wind speed as predictor are reported, since it shows good results based on NMC–statistics and because it is observable by radiosondes.

2 Two test cases for bad and fair weather

The same test cases of *bad* and *fair* weather over Central Europe are selected as in the previous report (Hess 2004) for this follow–on study. The first period

is 3–9 August 2003 and shows a large high pressure area with low winds and high surface temperatures. The other period is 6–12 January 2004 with strong westerly winds and lots of rain.

2.1 Validation with radiosonde departures

Error statistics of radiosonde temperature departures are computed for both periods. Only radiosondes of good quality are gathered that had been operationally used for 4D-Var at ECMWF. The same is true for all latter radiosonde statistics. The vertical distribution of rms temperature departures and the correlations with the 500 hPa pressure level are displayed in Fig. 1 for radiosondes valid at 0 UTC. Consistently with the NMC-method, the departures are smaller for the period in summer than for that in winter, although the difference is much smaller. (The rms difference for 500 hPa is about 0.55 K in summer and 0.75 K in winter, while it was about 0.3 K respectively 1.5 K for the NMC-statistics.) The correlations with the 500 hPa level are sharper for the summer case and are in a good agreement with the results bases on the NMC-method especially for the 500–700 hPa correlations. Also the negative correlations with 200–250 hPa are much more pronounced for the winter period.¹

For radiosondes valid at 12 UTC the results are very similar, see Fig. 2. This shows that the sampling is large enough to provide reliable statistics and that there are no qualitative differences between day and night.

Also in McNally (2000) the standard deviations of 500 hPa (and also of 700 hPa) of radiosonde-minus-background departures for the northern hemisphere ($60^{\circ}N$ – $40^{\circ}N$) were found slightly smaller in summer than in winter (about 0.90 K versus 0.95 K), specific weather conditions were not taken into account. In both cases the standard deviations of that study are slightly larger than the rms differences shown in Fig. 1. The means are very small in general, compare Fig. 4. One reason for that could be that the data of the study McNally (2000) is based on the year 1995/1996 and forecasts as well

¹In order to compute the vertical correlations, the temperature departures have been binned into the given pressure levels. The average of each bin is then used for further error statistics. The given number of observations represent the number of radiosondes therefore rather than the number of reported observations. Because of this averaging the presented rms errors decrease compared the to original statistics.

as radiosonde data has improved since then, another reason could be that the domain is the northern hemisphere, whereas the domain used here so far is restricted to Central Europe, an area where the quality of the forecast is rather high. The statistics based on north hemisphere samples below (see Figs. 6 and 7) show a rms value of about 0.8 K, which is slightly larger than the values for Europe as well.

How can we explain the quantitative discrepancy in the rms statistics between radiosonde departures and the NMC–method that is based on forecast differences? First of all it should be clarified that the sizes of the radiosonde departures are not to be compared to the 48–24 h forecast differences. These forecast ranges are chosen rather deliberately and should be scaled to the range of the short term forecast that provides the first guess.

It is noticeable, however, that the NMC–estimates of forecast error are much larger than the radiosonde estimates for the winter period,

In order to assess the radiosonde departures correctly, observation and representativity errors have to be taken into account with an assumed size of 0.76 K in the 4D–Var of ECMWF. This suggests that observation and representativity errors of the radiosondes dominate the summer statistics and that the actual forecast error is much smaller. The *analysis* departures (which are deliberately computed) are only slightly smaller than the background departures (below 250 hPa, hardly at all for 0 UTC), which also supports that observation and representativity errors are dominating in this case.

In winter the rms of the NMC–method at 500 hPa is very large compared to the radiosonde departures. The reason could be that the NMC–method is based on forecast differences and may include forecast errors of opposite sign that dominate the rms statistics.

2.2 Validation with satellite departures

Additional to radiosondes also satellite radiances are used to validate the theory of different forecast error structures for different synoptical situations. Departures of AMSU–A radiances of NOAA 16 are computed and the vertical distribution of rms differences and correlation with Channel no 6 are presented in Fig. 3. Channel no 6 has its highest sensitivity at about 400 hPa

whereas Channel no 5 peaks at about 700 hPa with considerable impact from the surface emissivity.

Again, for the summer period the departures are smaller and the correlations are sharper. This is consistent with the findings for the radiosondes. The rms differences are small in general, see Tab. 1, noticeable smaller than the assumed observation errors of 0.25 K for both channels. Because of the averaging of the broad weighting functions, the microwave departures are not quantitatively comparable to the in situ measurements of the radiosondes. Moreover, the sensitivity of Channel no 5 (and to a small extent also of Channel no 6) to the surface emission may affect the statistics. Because of the broad and overlapping weighting functions, the sizes of correlations are not comparable to the radiosonde departures. Qualitatively however the signal is consistent.

| Channel no | Summer | | Winter | |
|------------|---------|---------|---------|---------|
| | RMS [K] | COR [1] | RMS [K] | COR [1] |
| 5 | 0.20 | 0.22 | 0.25 | 0.37 |
| 6 | 0.15 | | 0.18 | |

Table 1: *RMS and correlation of departures of Channels AMSU-A no 5 and 6 of NOAA-16 for the summer and winter period in the northern hemisphere. Observations are valid around 0 UTC. Vertical distribution of values and sample sizes are given in Fig. 3.*

3 Wind speed as global predictor

The results of Sec. 2 are consistent with those given in the previous report (Hess 2004) and support the idea that the vertical error structures depend considerably on the actual synoptic situation. The next step is to prescribe these error structures in an objective way depending on suitable parameters that define the actual weather regime. In other words, the forecast errors need to be parameterised by suitable predictors.

Wind speed has been found a good predictor in order to separate different error structures in the previous study. Since it is directly observed by

radiosondes (e. g. in contrast to vorticity) it is chosen for first tests of parameterisations.

NMC-estimates of the 500 hPa temperature forecast errors are binned according to analysed wind velocity. The means and standard deviation of the bins are displayed in Fig. 4. In general, the mean errors are very small with a tendency for larger values in case of high winds. The standard deviations increase considerably from 0.3 to 0.8 K in an almost linear manner.

Figure 5 shows corresponding autocorrelations of the temperature errors. The 500–700 hPa correlations of temperature differences are positive in general and increase with wind speed from about 0.3 K for calm wind to 0.6 K for 50 m/s. The 500–300 hPa correlations are negative and decrease for the same range of wind speed from about 0.35 K to 0.65 K. In both cases the absolute values increase in an approximately linear or logarithmic shape. The statistics are smooth and the sampling of these statistics based on half a year of data can be considered large enough in order to provide significant results.

3.1 Validation with radiosondes

The idea to use wind speed as predictor for vertical error structures is again validated with radiosonde departures. Table 2 presents an overview of 500 hPa temperature departures of radiosondes and correlations with the 700 hPa pressure level. The same periods in winter and summer are selected as in Sec. 2, but the domain in question is the full northern hemisphere north of 20°N.

In general, the radiosonde statistics do not support the idea of using wind speed as a predictor for 500 hPa temperature forecast errors or temperature error correlations between 500 hPa and 700 hPa. The rms values are almost stable at 0.8 K for any regime of wind velocity. The correlations are even larger for smaller wind speeds than for higher. In winter the sampling of calm winds below 10 m/s is very small and the error measures are not evaluated therefore, the same is true for winds exceeding 25 m/s in summer.

When comparing the errors measures of summer and winter for the same wind speeds (smaller 15 m/s or larger 15 m/s), the correlations are almost twice as large for the winter period. This clarifies that there should be more important predictors to parameterise the covariances than wind speed.

The inconsistency that low wind speed leads to larger correlations in the radiosonde statistics is not understood and need further clarification.

| Wind speed [m/s] | Summer | | Winter | |
|------------------|---------|---------|---------|---------|
| | RMS [K] | COR [1] | RMS [K] | COR [1] |
| <5 | 0.81 | 0.21 | | |
| <10 | 0.83 | 0.09 | | |
| <15 | 0.83 | 0.11 | 0.79 | 0.21 |
| >15 | 0.82 | 0.09 | 0.85 | 0.15 |
| >25 | | | 0.85 | 0.16 |

Table 2: *RMS of 500hPa radiosonde departures and autocorrelation with 700hPa pressure level for summer and winter period (3–9 Aug 2003 resp. 6–12 Jan 2004) in the northern hemisphere sampled for different observed wind speed limits. Voids in case of sample size below 400 radiosondes. Vertical distribution of values and sample sizes are given in Figs. 6 and 7.*

3.2 Vertical distribution of radiosonde departures

Table 2 provides an overview, more detailed information for the vertical distributions of the radiosonde departures and their autocorrelations is presented in the following.

Figure 6 relates the samples of calm winds with high winds for the summer period. Although the temperature departures at 500 hPa are almost the same for calm and high winds, the errors of other levels up to 150 hPa are significantly larger by up to a quarter of a Kelvin in case of high winds. Only above 150 hPa the departures of the calm wind sample become larger. Not only the 500–700 hPa correlation is smaller for the high wind case, also correlations up to about 150 hPa are significantly smaller for high winds.

Figure 7 compares calm and high winds for the selected period in winter. Similarly to Fig. 6, the 500 hPa temperature departures are of almost same size for both wind speed samples, however the departures are larger by about 0.15 K between 300 hPa and 30 hPa in the high wind case. The correlations are again smaller for high winds for levels up to about 250 hPa.

To sum up it can be said, that there is some dependency of vertical radiosonde departures on wind speed on. However the signal is small for the 500 hPa

pressure level and 500-700 hPa correlation we focused on so far and it is much smaller than the NMC-statistics promised.

4 Conclusions

From this rather short visiting scientist mission a number of conclusions can be drawn or at least considered. In general all results are based on large statistical sample sizes that should provide significant results (half a year of data for the NMC-method and one week of radiosondes with more than 400 single accents for each given statistical value). NMC-estimates of forecast errors for different synoptic situations are validated using radiosonde departures. In this way both methods of forecast error estimation are compared and weaknesses are found for both methods. But also further details on the variable (flow dependent) vertical error structures are obtained that give motivation for further studies.

1. In the summer period with relatively small forecast errors the NMC-estimates of 500 hPa temperature error are much smaller than the statistics based on radiosonde data. In case of small forecast errors observation and representativity errors may dominate the radiosonde statistics and lead to an overestimation.
2. Large forecast errors in winter on the other hand might be overestimated by the NMC-method because of phase errors and other errors of opposite sign that dominate the statistics.
3. The NMC-method pretends a good dependency of forecasts errors on wind speed whereas this dependency is much smaller for radiosonde statistics. It is accepted that the NMC-method has problems in areas with few observations. The shorter forecasts are not significantly improved from the additional observations compared to the longer forecasts they are compared with. This results in a too small variability that is considered forecast error in the NMC-method. A similar effect may take place for observations in areas with little advection. The information is not distributed downstream and these areas are improved much less by the additional observations.

4. In almost any case the analysis departures show larger correlations than the background departures, see Figs. 6 and 7. Since the observation errors of radiosondes are specified vertically uncorrelated, this suggests that the used vertical background error correlations of 4D-Var are too broad.
5. It is confirmed with observations (radiosondes and AMSU-A radiances), that vertical error correlations depend to a large extent on the actual weather scenario. The dependency on wind speed is less important than anticipated, a seasonal effect might play an important role, which was demonstrated already in McNally (2000). Parameterising the vertical error structures with wind speed is therefore less attractive than the NMC-method promises at first glance, although some dependency on the vertical structures of forecast errors exists. To a large extent the dependency of forecast error on wind speed seems to be an artifact of the NMC-method.
6. The occurrence of large and broad vertically coupled error structures with negative correlations between troposphere and stratosphere that appear in *bad* weather conditions in winter can be explained with misplacements of extra-tropical features. A parameter would be required that measures the probability of the displacement of ridges, troughs, and cyclonal currencies. Vorticity would be the obvious choice for further investigations.

5 References

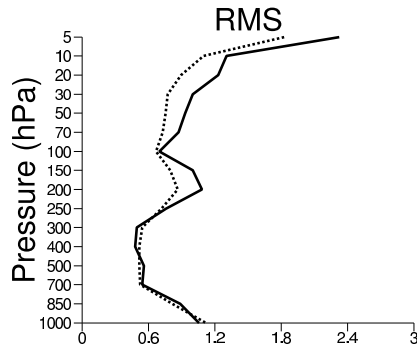
Hess, R.: *The specification of background error covariances for radiance assimilation*, NWP SAF Visiting Scientist Report (2004)

McNally, A. P.: *Estimates of short-range forecast-temperature error correlations and the implication for radiance-data assimilation*, Q. J. R. Meteorol. Soc. (2000), **126**, pp. 361–373

McNally, A. P.: *A note on the occurrence of cloud in meteorologically sensitive areas and the implications for advanced infrared sounders*, Q. J. R. Meteorol. Soc. (2002), **128**, pp. 2251–2556

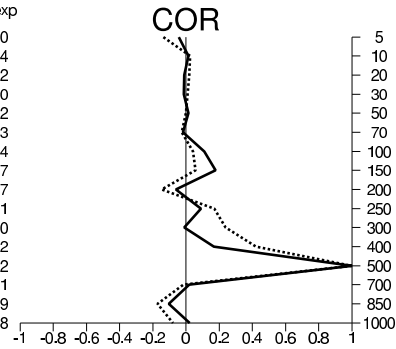
Parrish, D. F. and Derber, J. C.: *The National Meteorological Center's Spectral Statistical Interpolation Analysis system*, Mon.Weather Rev. (1981), **120**, pp. 1747–1763

exp:0001 v 2003080300-2003080900(24)
 TEMP-T areaNSEW= 60/ 40/ 20/ -20
 used T

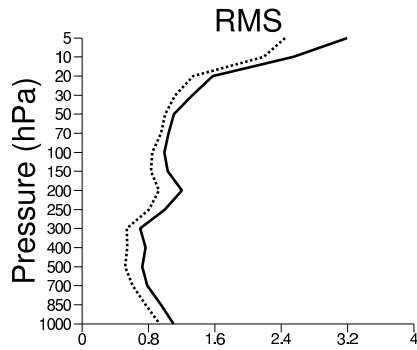


nobsxp
 60
 194
 292
 330
 342
 353
 374
 377
 377
 381
 380
 382
 382
 381
 379
 368

— background departure o-b
 - - - analysis departure o-a



exp:0001 v 2004010600-2004011200(24)
 TEMP-T areaNSEW= 60/ 40/ 20/ -20
 used T



nobsxp
 19
 65
 98
 199
 282
 303
 320
 333
 337
 337
 341
 347
 349
 348
 345
 336

— background departure o-b
 - - - analysis departure o-a

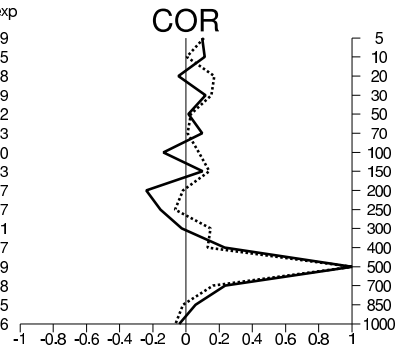
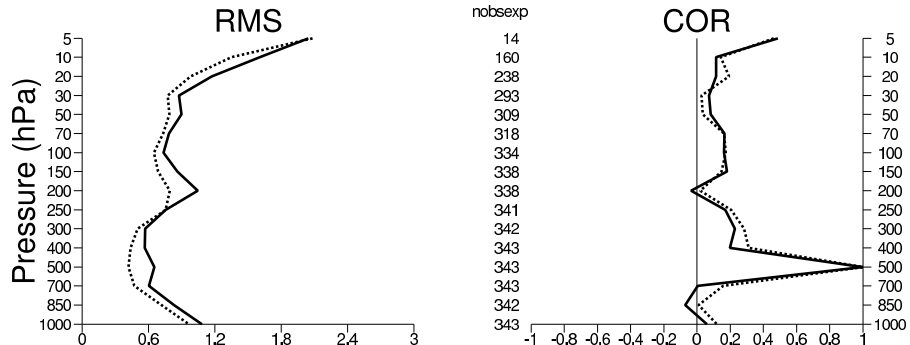


Figure 1: Error statistics for summer (top) and winter (bottom) period: Displayed are rms error of radiosonde temperature departures and autocorrelation with 500hPa level. First guess departures are in solid lines, analysis departures from ECMWF 4D-Var are dashed. Radiosondes are valid for 0 UTC.

exp:0001 v 2003080312-2003080912(24)
 TEMP-T areaNSEW= 60/ 40/ 20/ -20
 used T

———— background departure o-b
 analysis departure o-a



exp:0001 v 2004010600-2004011200(24)
 TEMP-T areaNSEW= 60/ 40/ 20/ -20
 used T

———— background departure o-b
 analysis departure o-a

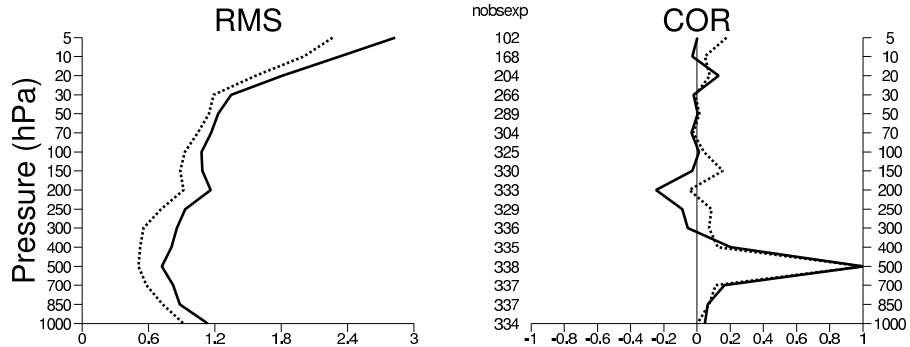
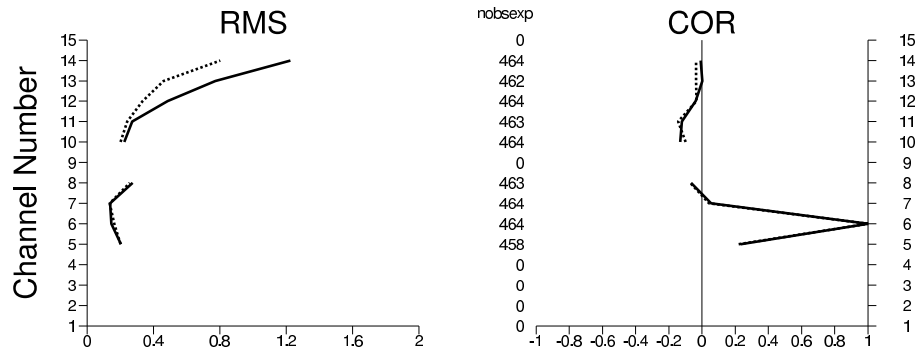


Figure 2: Same as Fig. 1 but for radiosondes valid for 12 UTC.

exp:0001 v 2003080300-2003080900(24) ———— background departure o-b
 TOVS-1C noaa-16 AMSU-A Tb areaNSEW= 60/ 40/ 20/ -20..... analysis departure o-a
 used Tb noaa-16 amsu-a



exp:0001 v 2004010600-2004011200(24) ———— background departure o-b
 TOVS-1C noaa-16 AMSU-A Tb areaNSEW= 60/ 40/ 20/ -20..... analysis departure o-a
 used Tb noaa-16 amsu-a

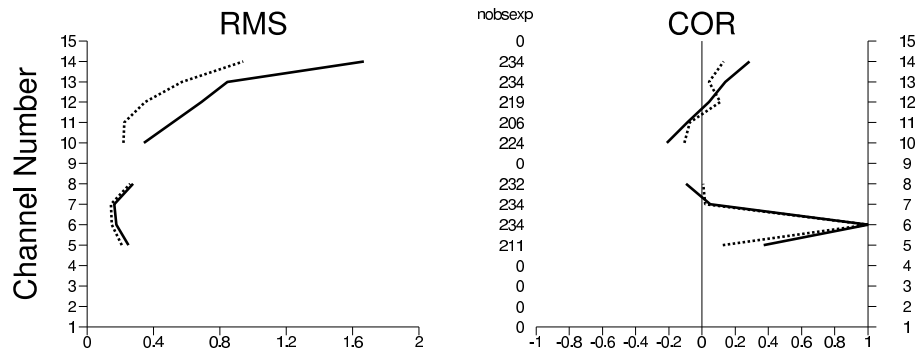


Figure 3: Error statistics for summer (top) and winter (bottom) period in radiance space of AMSU-A: Displayed are rms error of AMSU-A temperature departures and autocorrelation with Channel no 6. First guess departures are in solid lines, analysis departures from ECMWF 4D-Var are dashed. Radiances are valid around 0 UTC.

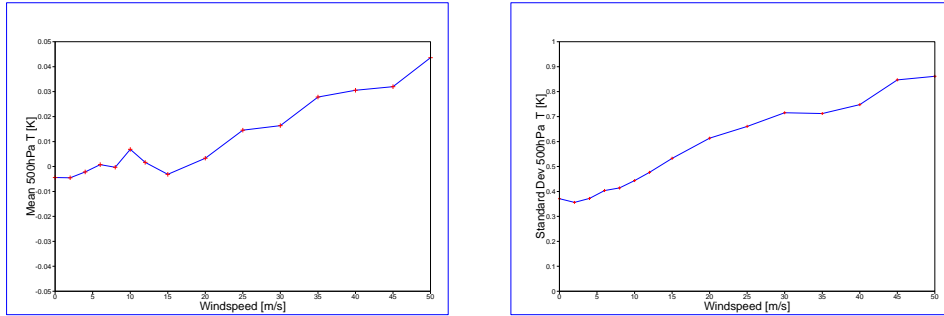


Figure 4: Mean and standard deviation of 500hPa temperature errors as derived from the NMC-method binned according to wind velocity. The sampling consists of global values from April to September 2003.

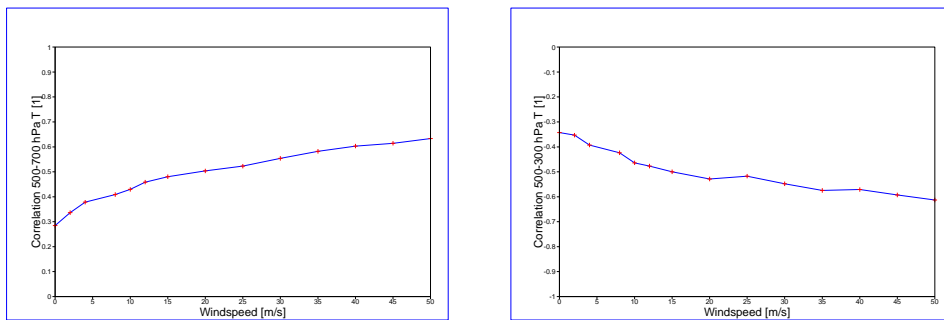
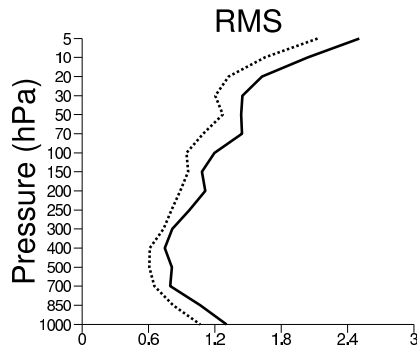


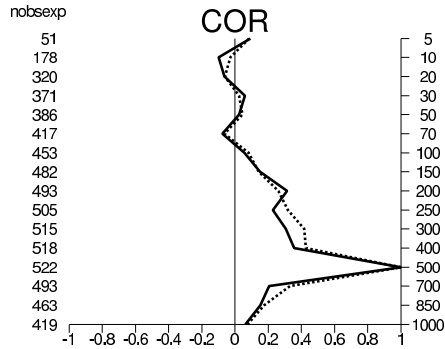
Figure 5: As Fig. 4 but for 500–700 hPa (left) and 500–300 hPa (right) temperature correlations.

exp:0001 v 2003080300-2003080900(24)
 TEMP-T N.Hemis v<5m/s
 used T

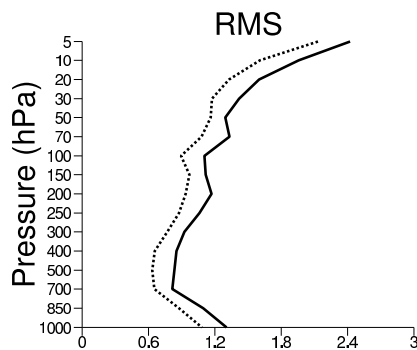


nobsxp
 51
 178
 320
 371
 386
 417
 453
 482
 493
 505
 515
 518
 522
 493
 463
 419

———— background departure o-b
 analysis departure o-a

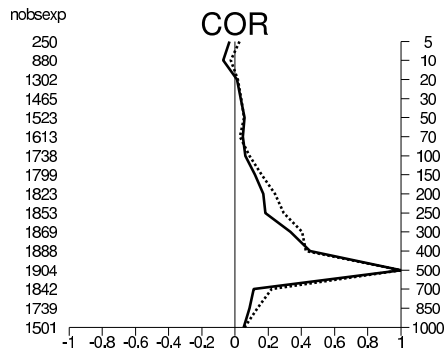


exp:0001 v 2003080300-2003080900(24)
 TEMP-T N.Hemis v<15m/s
 used T

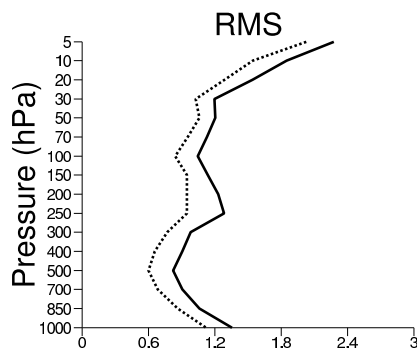


nobsxp
 250
 880
 1302
 1465
 1523
 1613
 1738
 1799
 1823
 1853
 1869
 1888
 1904
 1842
 1739
 1501

———— background departure o-b
 analysis departure o-a



exp:0001 v 2003080300-2003080900(24)
 TEMP-T N.Hemis v>15m/s
 used T



nobsxp
 79
 255
 315
 357
 366
 386
 408
 413
 423
 424
 430
 433
 436
 434
 419
 375

———— background departure o-b
 analysis departure o-a

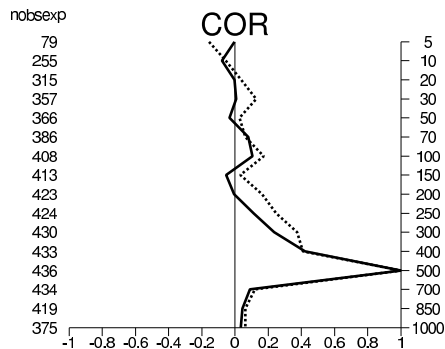
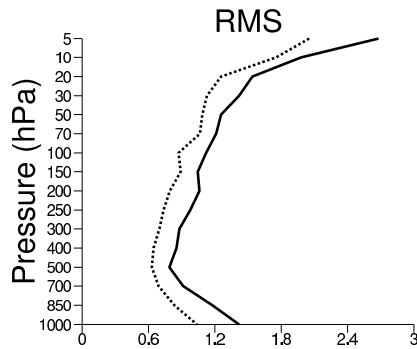


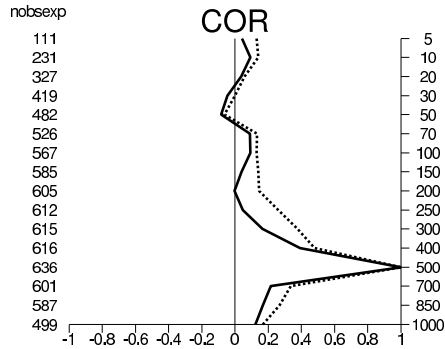
Figure 6: Vertical distribution of radiosonde temperature departures temperature and autocorrelation with 500 hPa level for northern hemisphere summer period for 0 UTC radiosondes. Observed wind speed less than 5 m/s on top, less than 15 m/s below, and wind speed higher than 15 m/s at the bottom. Background departures in solid, analysis departures in dotted lines.

exp:0001 v 2004010600-2004011200(24)
 TEMP-T N.Hemis v<15m/s
 used T

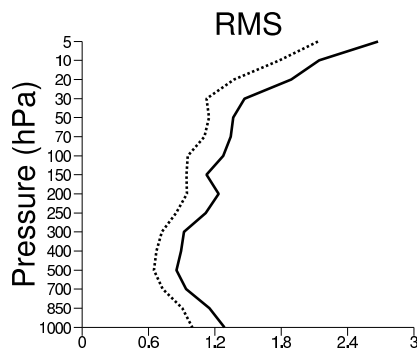


nobsxp
 111
 231
 327
 419
 482
 526
 567
 585
 605
 612
 615
 616
 636
 601
 587
 499

— background departure o-b
 analysis departure o-a

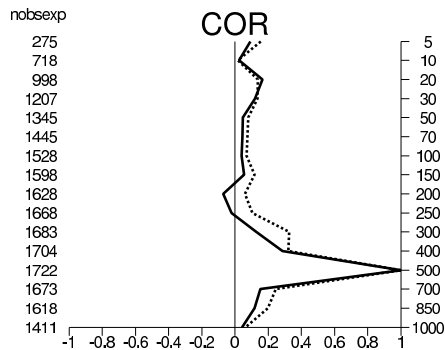


exp:0001 v 2004010600-2004011200(24)
 TEMP-T N.Hemis v>15m/s
 used T

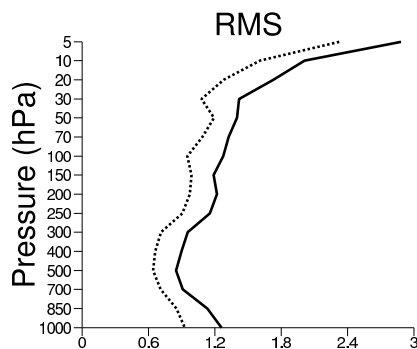


nobsxp
 275
 718
 998
 1207
 1345
 1445
 1528
 1598
 1628
 1668
 1683
 1704
 1722
 1673
 1618
 1411

— background departure o-b
 analysis departure o-a



exp:0001 v 2004010600-2004011200(24)
 TEMP-T N.Hemis v>25m/s
 used T



nobsxp
 129
 348
 451
 537
 591
 639
 673
 707
 716
 731
 738
 751
 756
 747
 730
 676

— background departure o-b
 analysis departure o-a

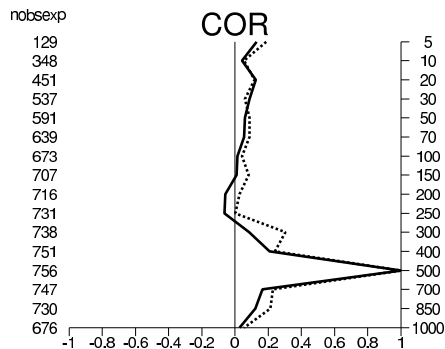


Figure 7: Similar to Fig. 6, but for winter period; wind speed less than 15 m/s on top, more than 15 m/s below, and more than 25 m/s at the bottom.